

Coherent pion electroproduction on the deuteron in the $\Delta(1232)$ resonance region*

Thomas Ebertshäuser and Hartmuth Arenhövel

Institut für Kernphysik, Johannes Gutenberg-Universität, D-55099 Mainz, Germany

Coherent pion electroproduction on the deuteron is studied in the $\Delta(1232)$ resonance region in the impulse approximation, i.e., neglecting pion rescattering and two-body effects. The elementary reaction on the nucleon is described in the framework of an effective Lagrangian approach including the dominant $P_{33}(1232)$ resonance and the usual background terms of the Born contributions for π^0 production. We have studied the influence of these different contributions on the various structure functions which determine the unpolarized exclusive differential cross section in a variety of kinematic regions.

I. INTRODUCTION

Electromagnetic meson production off nuclei has become a major topic in medium energy physics. It offers the possibility to study the elementary production process in a strong interacting medium thus allowing to investigate in detail, for example, possible modifications of the elementary production process due to the surrounding medium. Another, though complementary aspect is to study the production on the neutron, which as a free process is in most cases not accessible. One exception is the radiative π^+ capture on the proton. Thus it is not surprising that in recent years, photo- and electroproduction of π and η mesons on nuclei have been studied intensively (see for example recent work in [1,2]) with particular emphasis on testing the elementary production amplitude of the neutron. This renewed interest has been triggered primarily by the significant improvement on the quality of experimental data obtained with the new generation of high-duty cycle electron accelerators like, e.g., ELSA in Bonn and MAMI in Mainz [3–6].

Pion photo- and electroproduction on the deuteron is especially interesting with respect to the above mentioned two complementary aspects since first it allows one to study this reaction on a bound nucleon in the simplest nuclear environment so that one can take into account medium effects in a reliable manner, at least in the nonrelativistic domain. Secondly, it provides important information on this reaction on the neutron. In view of this latter aspect, the deuteron is often considered as a neutron target assuming that binding effects can be neglected to a large extent. Most of the theoretical work has concentrated on the photo reaction (see Refs. [7–12] where also references to earlier work can be found) while very few studies of the corresponding electroproduction process exist. The latter has been considered briefly in [8] with respect to target asymmetries for two specific kinematic settings, while in [13] the role of exchange contributions in the longitudinal form factor near threshold has been investigated. But a systematic study is still missing.

The aim of the present work is to initiate such a systematic study of the $d(e, e' \pi^0)d$ reaction from threshold through the $\Delta(1232)$ resonance similar to what has been done already for the corresponding photo production process [10,11]. As a first step, we will restrict ourselves in this work to the impulse approximation (IA), where the production takes place at one nucleon only, in order to study details of the elementary reaction amplitude and, furthermore, we are interested mainly in the Δ resonance region. Because close to threshold the elementary operator used in this work does not give a realistic description. With respect to the elementary production operator, we follow essentially the treatment of [10,11] supplementing the transverse current by charge and longitudinal contributions and including electromagnetic form factors at the elementary photon vertices. Any pion rescattering effects or two body contributions to the general current operator are neglected completely. Their treatment will be deferred to a later study.

The paper is organized as follows: In the next section we present the theoretical framework for the coherent electroproduction process on the deuteron with definition of the structure functions which determine the differential cross section. Furthermore, we will briefly discuss a set of nonrelativistic amplitudes which form a basis for the expansion of the general T -matrix with appropriate invariant functions as coefficients. A derivation of this set is given in the Appendix. Then we discuss in Sect. III the impulse approximation which serves as a calculational basis for the evaluation. In this section we also outline the elementary operator used in this work. In Sect. IV we present and discuss the results for the structure functions and form factors in various kinematic regions. Finally, we give a brief summary and an outlook.

*Supported by the Deutsche Forschungsgemeinschaft (SFB 443)

II. GENERAL FORMALISM

In this section we will briefly outline the formalism of coherent electroproduction of neutral pions on deuterium which in the one-photon approximation can be described as the absorption of a virtual photon, i.e.

$$\gamma^*(k) + d(p) \rightarrow d(p') + \pi^0(q), \quad (1)$$

where the momenta of initial virtual photon and deuteron are denoted by k and p , and the final deuteron and pion momenta by p' and q , respectively. We will consider this reaction in the photon-deuteron (γ^*d) c.m. frame. There we choose the z -axis along the virtual photon momentum ($\vec{e}_z = \hat{k} = \vec{k}/k$), the y -axis parallel to $\vec{k} \times \vec{q}$ and the x -axis such as to form a right handed system. Thus the outgoing π meson is described by the spherical angles ϕ and θ with $\cos \theta = \hat{q} \cdot \hat{k}$.

In the one-photon approximation the differential cross section for the production process using unpolarized electrons and an unpolarized target is given by

$$\frac{d\sigma}{dk_2^{lab} d\Omega_e^{lab} d\Omega_{\pi^0}^{c.m.}} = c \{ \rho_L f_L + \rho_T f_T + \rho_{LT} f_{LT} \cos \phi + \rho_{TT} f_{TT} \cos 2\phi \}. \quad (2)$$

Here c is a kinematic factor

$$c(k_1^{lab}, k_2^{lab}) = \frac{\alpha}{6\pi^2} \frac{k_2^{lab}}{k_1^{lab} k_\nu^4}, \quad (3)$$

where $k_{1/2}^{lab}$ denote incoming and scattered electron momenta in the lab frame, α the fine structure constant, and $k_\nu^2 = k_0^2 - \vec{k}^2$ the four momentum transfer squared ($k = k_1 - k_2$).

$$\rho_L = -\beta^2 k_\nu^2 \frac{\xi^2}{2\eta}, \quad \rho_{LT} = -\beta k_\nu^2 \frac{\xi}{\eta} \sqrt{\frac{\xi + \eta}{8}}, \quad (4)$$

$$\rho_T = -\frac{1}{2} k_\nu^2 \left(1 + \frac{\xi}{2\eta}\right), \quad \rho_{TT} = k_\nu^2 \frac{\xi}{4\eta}, \quad (5)$$

with

$$\beta = \frac{|\vec{k}^{lab}|}{|\vec{k}^c|}, \quad \xi = -\frac{k_\nu^2}{(\vec{k}^{lab})^2}, \quad \eta = \tan^2\left(\frac{\theta_e^{lab}}{2}\right), \quad (6)$$

where θ_e^{lab} denotes the electron scattering angle in the lab system and β expresses the boost from the lab system to the frame in which the T -matrix is evaluated and \vec{k}^c denotes the momentum transfer in this frame.

The structure functions in (2) are given in terms of the reduced reaction matrix elements $t_{m'\lambda m}$ which are defined by the general T -matrix element of the current operator in the c.m. frame

$$\begin{aligned} T_{m'\mu m}(W_{\gamma^*d}, \theta, \phi) &= -\sqrt{\frac{\alpha |\vec{q}| E_k^d E_q^d}{4\pi m_d W_{\gamma^*d}}} \langle 1m' | \tilde{J}_\mu(\vec{k} - \vec{q}) | 1m \rangle \\ &= e^{i(\mu+m)\phi} t_{m'\mu m}(W_{\gamma^*d}, \theta), \end{aligned} \quad (7)$$

where the initial and final deuteron spin projections are denoted by m and m' , respectively, the photon polarization by μ , and initial and final deuteron c.m. energies by E_k^d and E_q^d , respectively, with $E_p^d = \sqrt{m_d^2 + \vec{p}^2}$ and m_d as deuteron mass. Furthermore, W_{γ^*d} denotes the invariant mass of the γ^*d system and k and q the photon and π^0 momenta, respectively, in the γ^*d c.m. system.

In detail one has

$$\begin{aligned} f_L &= \sum_{m',m} \Re e(t_{m'0m}^* t_{m'0m}), & f_T &= 2 \sum_{m',m} \Re e(t_{m'1m}^* t_{m'1m}), \\ f_{LT} &= 4 \sum_{m',m} \Re e(t_{m'0m}^* t_{m'1m}), & f_{TT} &= 2 \sum_{m',m} \Re e(t_{m'-1m}^* t_{m'1m}). \end{aligned} \quad (8)$$

The structure functions are functions of the invariant mass W_{γ^*d} , the squared three momentum transfer $(\vec{k}^{c.m.})^2$ and the angle θ between \vec{k} and the momentum \vec{q} of the outgoing pion, i.e.

$$f_\alpha = f_\alpha(W_{\gamma^*d}, (\vec{k}^{c.m.})^2, \theta) \quad \text{for } \alpha \in \{L, T, LT, TT\}. \quad (9)$$

The inclusive cross section obtained by integrating over the pion angles is determined by the longitudinal and transverse form factors F_L and F_T , respectively, which are defined by

$$F_{L/T}(W_{\gamma^*d}, (\vec{k}^{c.m.})^2) = \int d\Omega_q f_{L/T}(W_{\gamma^*d}, (\vec{k}^{c.m.})^2, \theta). \quad (10)$$

In analogy to the CGLN-amplitudes of e.m. pion production on a nucleon, a set of 13 basic covariant amplitudes Ω_α has been derived in [14] which allow a representation of the T -matrix as a linear superposition of these amplitudes with invariant functions $F_\alpha(s, t, u)$ as coefficients depending on the Mandelstam variables only

$$T = \sum_\alpha F_\alpha(s, t, u) \Omega_\alpha. \quad (11)$$

An equivalent nonrelativistic set of transverse $\mathcal{O}_{T,\beta}$ and longitudinal $\mathcal{O}_{L,\beta}$ operators has also been given in [14] which is listed in Table I explicitly. Here \vec{S} denotes the spin operator for $(S=1)$ -particle and $S^{[2]}$ the corresponding tensor operator defined by

$$S^{[2]} = [S^{[1]} \times S^{[1]}]^{[2]} \quad (12)$$

in the notation of Fano and Racah [15]. The operators $\mathbb{1}_3$, $S^{[1]}$, and $S^{[2]}$ form a complete set of (3×3) -matrices in $(S=1)$ -space. Furthermore, in Table I \hat{k} and \hat{q} denote corresponding unit vectors and with $\hat{k} = k^{[1]}$

$$k^{[2]} = [k^{[1]} \times k^{[1]}]^{[2]}. \quad (13)$$

In the Appendix, we give an independent proof that this set forms a complete basis for the representation of the T -matrix for the process under consideration. In the present nonrelativistic framework this set is more appropriate and one can represent the T -matrix correspondingly

$$T_{m'\mu m} = \delta_{|\mu|1} \sum_{\beta=1}^9 f_\beta^T (\mathcal{O}_{T,\beta})_{m'\mu m} + \delta_{\mu 0} \sum_{\beta=1}^4 f_\beta^L (\mathcal{O}_{L,\beta})_{m'\mu m} \quad (14)$$

with appropriate functions $f_\beta^{L/T}$. Any contribution to the reaction can be expanded in terms of these amplitudes. In the present work, however, where we restrict ourselves to the pure impulse approximation (IA), we will evaluate directly the various terms of the elementary production operator on the nucleon without separating explicitly the various operator contributions.

III. THE IMPULSE APPROXIMATION

In the IA, the π^0 production takes place at one nucleon while the other acts merely as a spectator. Thus the basic diagrams of the IA consisting of a resonance and two Born terms are the ones depicted in Fig. 1. Consequently, the production operator $\hat{t}_{\gamma\pi^0}^d$ for the reaction on the deuteron which governs the T -matrix in the c.m. frame of virtual photon and deuteron

$$T_{m'\mu m}(W_{\gamma^*d}, \theta, \phi) = \langle -\vec{q}, m' | \hat{t}_{\gamma\pi^0}^d(W_{\gamma^*d}) | -\vec{k}, m\mu \rangle, \quad (15)$$

is obtained from the elementary operator $\hat{t}_{\gamma^*\pi^0}$ by

$$\hat{t}_{\gamma^*\pi^0}^d(W_{\gamma^*d}) = \hat{t}_{\gamma^*\pi^0}^{(1)}(W_{\gamma^*N}) \otimes \mathbb{1}^{(2)} + \mathbb{1}^{(1)} \otimes \hat{t}_{\gamma^*\pi^0}^{(2)}(W_{\gamma^*N}), \quad (16)$$

where the upper index in brackets refers to the nucleon on which the operator acts. Off-shell effects will be neglected. The invariant mass of the γ^*N system is denoted by W_{γ^*N} . The assignment of W_{γ^*N} will be discussed below.

Explicitly one finds

$$T_{m'\mu m} = 2 \sum_{m'_s, m_s} \int d^3p \psi_{m'_s m'}^* \left(\vec{p} - \frac{\vec{q}}{2} \right) \langle \vec{p} - \vec{q}; 1m'_s, 00 | \hat{t}_{\gamma^* \pi^0}^{(1)} | \vec{p} - \vec{k}; 1m_s, 00 \rangle \psi_{m_s m} \left(\vec{p} - \frac{\vec{k}}{2} \right), \quad (17)$$

where $\langle \vec{p}'; 1m'_s, 00 | \hat{t}_{\gamma^* \pi^0}^{(1)} | \vec{p}; 1m_s, 00 \rangle$ denotes the elementary t -matrix for initial and final nucleon momentum \vec{p} and \vec{p}' , respectively, evaluated between two-nucleon spin and isospin wave functions $|1m'_s, 00\rangle = |(\frac{1}{2}\frac{1}{2})1m'_s, (\frac{1}{2}\frac{1}{2})00\rangle$ and $|1m_s, 00\rangle$. Furthermore, $\psi_{m_s m}(\vec{p})$ denotes the intrinsic part of the deuteron wave function in momentum space projected onto $|1m_s, 00\rangle$

$$\psi_{m_s m}(\vec{p}) = \sum_{l=0,2} \sum_{m_l} (lm_l 1m_s | 1m) u_l(p) Y_{l, m_l}(\hat{p}), \quad (18)$$

where $\vec{p} = \frac{1}{2}(\vec{p}_1 - \vec{p}_2)$ denotes the relative momentum of the two nucleons in the deuteron.

For the evaluation of (17) one has to specify the elementary operator $\hat{t}_{\gamma^* \pi^0}$ for the reaction $\gamma^* + N \rightarrow \pi^0 + N$. As already mentioned, we will follow the treatment in [10,11] for the coherent photoproduction process taking into account the Δ resonance contribution and as background the Born terms from the direct and crossed nucleon pole diagrams, denoted “ NP ” and “ NC ”, respectively, in Fig. 1, i.e.

$$\hat{t}_{\gamma^* \pi^0} = \hat{t}_{\gamma^* \pi^0}^{(\Delta)} + \hat{t}_{\gamma^* \pi^0}^{(NP)} + \hat{t}_{\gamma^* \pi^0}^{(NC)}. \quad (19)$$

We will first consider the Born terms whose contributions are given by

$$\hat{t}_{\gamma^* \pi^0}^{(NP)}(z) = v_{\pi^0 N}^\dagger G^{(NP)}(z) v_{\gamma^* N}, \quad (20)$$

$$\hat{t}_{\gamma^* \pi^0}^{(NC)}(z) = v_{\gamma^* N} G^{(NC)}(z) v_{\pi^0 N}^\dagger. \quad (21)$$

The vertex functions are

$$v_{\pi^0 N}^\dagger = -i \frac{f_\pi}{m_\pi} \vec{\sigma} \cdot \vec{q} \tau_0, \quad (22)$$

$$v_{\gamma^* N} = \epsilon_\nu(\mu) j_N^\nu(\vec{k}), \quad (23)$$

where $\epsilon_\nu(\mu)$ denotes the polarization vector of the virtual photon with helicity μ . As πN coupling constant we have chosen $\frac{f_\pi^2}{4\pi} = 0.08$, and the nucleon charge and current densities are given by the nonrelativistic expressions

$$\rho_N = \hat{e}, \quad (24)$$

$$\vec{J}_N = \frac{\hat{e}}{2m_N} (\vec{p}' + \vec{p}) + \frac{\hat{e} + \hat{\kappa}}{2m_N} i \vec{\sigma} \times \vec{k}, \quad (25)$$

with

$$\hat{e} = \frac{e}{2} (1 + \tau_0) F(k_\mu^2), \quad \hat{\kappa} = \frac{e}{2} (\kappa_p (1 + \tau_0) + \kappa_n (1 - \tau_0)) F(k_\mu^2). \quad (26)$$

Here e denotes the elementary charge and $\kappa_{n/p}$ the anomalous magnetic moment of neutron and proton, respectively. Furthermore, we have introduced a common e.m. form factor $F(k_\mu^2)$ for which we have chosen the dipole parametrization

$$F(k_\mu^2) = \left(1 - \frac{k_\mu^2}{0.71(\text{GeV})^2} \right)^{-2}. \quad (27)$$

The propagators of the direct and crossed terms are of the form

$$G^{(NP)}(z) = \frac{1}{z - E_{\vec{p}}^{(N)} + i\epsilon}, \quad G^{(NC)}(z) = \frac{1}{z - E_{\vec{p}}^{(N)} - E^{(\pi)} - \omega + i\epsilon}, \quad (28)$$

where $E^{(\pi)} = \sqrt{m_\pi^2 + \vec{q}^2}$ denotes the relativistic pion energy and $E_{\vec{p}}^{(N)} = m_N + \frac{\vec{p}^2}{2m_N}$ the nonrelativistic nucleon energy. For the resonance contribution

$$\hat{t}_{\gamma^*\pi^0}^{(\Delta)}(z) = v_{\pi^0 N\Delta}^\dagger G^{(\Delta)}(z) v_{\gamma^* N\Delta}, \quad (29)$$

we use for the $\gamma^* N\Delta$ vertex the dominant $M1$ contribution of the $N\Delta$ transition current

$$\rho_{\gamma^* N\Delta}^{M1} = eF(k_\mu^2) \frac{\tilde{G}_{\gamma N\Delta}^{M1}(E_\Delta)}{2m_N m_\Delta} i(\vec{\sigma}_{\Delta N} \times \vec{k}) \cdot \vec{p}_N \tau_{\Delta N,0}, \quad (30)$$

$$\vec{j}_{\gamma^* N\Delta}^{M1} = eF(k_\mu^2) \frac{\tilde{G}_{\gamma N\Delta}^{M1}(E_\Delta)}{2m_N} i\vec{\sigma}_{\Delta N} \times \vec{k}_{\gamma N} \tau_{\Delta N,0}, \quad (31)$$

neglecting the tiny $C2$ and $E2$ parts, because they are not expected to play a significant role in the pure impulse approximation where also other small effects are not considered. Here we use $m_\Delta = 1232$ MeV and

$$\vec{k}_{\gamma N} = \frac{m_N \vec{k} - \omega \vec{p}_N}{m_\Delta}, \quad (32)$$

and $E_\Delta = W_{\gamma^* N}$ is the Δ energy in its rest system. The $\gamma^* N\Delta$ coupling is taken as energy dependent and parametrized in the form [10]

$$\tilde{G}_{\gamma N\Delta}^{M1}(E_\Delta) = \begin{cases} \mu_{M1}(q_0(E_\Delta)) \exp[i\Phi_{M1}(q_0(E_\Delta))] & \text{if } E_\Delta > m_\pi + m_N, \\ \mu_0 & \text{else,} \end{cases} \quad (33)$$

where the different quantities are defined as

$$\mu_{M1}(q_0) = \mu_0 + \mu_2 \left(\frac{q_0}{m_\pi}\right)^2 + \mu_4 \left(\frac{q_0}{m_\pi}\right)^4, \quad (34)$$

$$\Phi_{M1}(q_0) = \frac{q_0^3}{a_1 + a_2 q_0^2}, \quad (35)$$

with $q_0(E_\Delta)$ as the on-shell pion momentum in this system, given by

$$E_\Delta = \sqrt{m_\pi^2 + q_0^2} + m_N + \frac{q_0^2}{2m_N}. \quad (36)$$

The parameters have been fixed by fitting the $M_{1+}^{3/2}$ multipole of pion photoproduction yielding the values $\mu_0 = 4.16$, $\mu_2 = 0.542$, $\mu_4 = -0.0757$, $a_1 = 0.185$ fm⁻³, and $a_2 = 4.94$ fm⁻¹ [10].

The $\pi^0 N\Delta$ vertex is given in the usual form

$$v_{\pi^0 N\Delta}^\dagger = -i \frac{f_\Delta}{m_\pi} F_\Delta(\vec{q}_{\pi N}^2) \vec{\sigma}_{N\Delta} \cdot \vec{q}_{\pi N} \tau_{N\Delta,0}, \quad (37)$$

with

$$\vec{q}_{\pi N} = \frac{m_N \vec{q} - E^{(\pi)} \vec{p}_N}{m_N + E^{(\pi)}}, \quad (38)$$

and the $N\Delta$ coupling constant $\frac{f_\Delta^2}{4\pi} = 1.393$. Here $\vec{\sigma}_{N\Delta}$ and $\tau_{N\Delta,0}$ denote the usual spin and isospin $N\Delta$ transition operators, respectively. The hadronic form factor is taken of dipole type with parameters also obtained in the above mentioned fit

$$F_\Delta(\vec{q}_{\pi N}^2) = \frac{\Lambda_\Delta^2 - m_\pi^2}{\Lambda_\Delta^2 + \vec{q}_{\pi N}^2}, \quad (39)$$

where $\Lambda_\Delta = 287.9$ MeV, and $m_\Delta^0 = 1315$ MeV. Finally, the Δ resonance propagator is of the form

$$G^{(\Delta)}(E_\Delta) = \frac{1}{E_\Delta - M_\Delta(E_\Delta) + \frac{i}{2}\Gamma_\Delta(E_\Delta)}, \quad (40)$$

where the energy dependent mass and width are given by

$$M_{\Delta}(E_{\Delta}) = m_{\Delta}^0 + \frac{f_{\Delta}^2}{12\pi^2 m_{\pi}^2} \wp \int_0^{\infty} \frac{dq' q'^4 F_{\Delta}^2(q'^2)}{\sqrt{m_{\pi}^2 + q'^2} (E_{\Delta} - \sqrt{m_{\pi}^2 + q'^2} - m_N - \frac{q'^2}{2m_N})}, \quad (41)$$

and

$$\Gamma_{\Delta}(E_{\Delta}) = \begin{cases} \frac{q_0(E_{\Delta})^3 m_N}{6\pi m_{\pi}^2 (\sqrt{m_{\pi}^2 + q_0(E_{\Delta})^2} + m_N)} f_{\Delta} F_{\Delta}^2(q_0(E_{\Delta})^2) & \text{if } E_{\Delta} > m_{\pi} + m_N, \\ 0 & \text{else.} \end{cases} \quad (42)$$

The elementary operator $\hat{t}_{\gamma^* \pi^0}^{(1)}$ is a function of the photon, nucleon and π^0 momenta \vec{k} , \vec{p} , and \vec{q} , respectively, the photon polarization μ , and of the invariant mass $W_{\gamma^* N}$ of the photon-nucleon subsystem. Implementing this operator into a bound system poses the problem of assigning an invariant mass $W_{\gamma^* N}$ for the struck or active nucleon. This question has been discussed in detail in [16] for coherent η photoproduction on the deuteron by studying various prescriptions. In this work we have adopted the spectator-on-shell assignment as in [10,11].

IV. RESULTS AND DISCUSSION

Having fixed the parameters of the π^0 production model for the elementary reaction on the nucleon, we have calculated the coherent reaction on the deuteron. The t -matrix elements of (17) have been evaluated numerically using Gauss integration in momentum space. As deuteron wave function, we have taken the one of the Bonn r -space potential in the parametrized form [17]. In order to test the numerical program, we have first calculated the differential and total cross sections at the photon point and compared the results to the one of [10] for which we obtained complete agreement. Since in electroproduction energy and momentum transfers can be varied independently in the spacelike region, we have chosen various cuts along constant energy or momentum transfer as shown in Fig. 2 for which we calculated the four structure functions. For the sets A, B and C we have fixed the momentum transfer k and varied the energy transfer ω , while for set D we have fixed ω and varied k . The set A at a moderate momentum transfer of $k^2 = 2 \text{ fm}^{-2}$ covers the region right above the production threshold up to the onset of the Δ -resonance. The sets B and C are cuts across the Δ -resonance for fixed three momentum transfers $k^2 = 5 \text{ fm}^{-2}$ and $k^2 = 10 \text{ fm}^{-2}$, respectively, while set D for a fixed energy transfer $\omega = 300 \text{ MeV}$ remains essentially above but close to the resonance region.

We will start the discussion of the structure functions with set A shown in Fig. 3. The longitudinal structure function f_L is almost not affected by the Δ resonance. This is a consequence of the assumed pure $M1$ excitation of the Δ leading to a completely transverse current in the Δ rest frame, so that any longitudinal contribution which arises when going to other frames are negligible. Therefore, this structure function is governed by the Born terms only. One readily notes a strong destructive interference between direct and crossed terms resulting in a small forward peaked angular distribution, except very close to threshold.

For the transverse structure function f_T one notices an increasing forward peaking of the total IA with increasing ω , except for the lowest energy transfer close to threshold where an almost symmetric forward backward peaking appears. At the lowest energy transfer, f_T is dominated by the Born terms displaying a constructive interference between direct and crossed contributions in sharp contrast to the findings for f_L . This different behaviour of the Born terms is easily understood from the structure of the corresponding operators and the sign of the propagators. For the longitudinal part, the operators of direct and crossed contributions have the same sign, while they differ in sign for most of the transverse operators which combined with the opposite signs of the propagators leads to the observed destructive, respectively, constructive behaviour. Close to threshold, the Δ contribution is small as expected. It shows a slight peaking around 90 degree. With increasing ω this peak moves more and more to forward angles. Also its relative size increases rapidly becoming dominant at the highest energy displayed. At the higher energies f_T is more than an order of magnitude bigger than f_L .

For the longitudinal-transverse interference structure function f_{LT} the Δ contribution yields a negative structure function of increasing size with increasing ω . The direct Born term interferes constructively in the forward direction while destructively at backward angles and the crossover moves more and more to smaller angles with increasing energy. The crossed Born contribution interferes destructively with both, Δ and direct Born terms, resulting in a positive structure function over a large forward angular range. The size of f_{LT} is comparable to f_L for the total contributions.

Finally, the transverse interference structure function f_{TT} receives a positive contribution from the Δ with a peak moving from about 90 degree near threshold to smaller angles, about 55 degree for the highest energy transfer. There is a strong destructive interference effect from the Born terms which even leads to a sign change near threshold, but their importance becomes smaller and smaller when approaching the Δ region. Its size is only a factor three smaller than f_T at the two highest ω values.

For the sets B and C at constant three momentum transfers of $k^2 = 5 \text{ fm}^{-2}$ and $k^2 = 10 \text{ fm}^{-2}$, respectively, we have chosen the four energy transfers ω in such a manner that pairwise they correspond to the same invariant energies $W_{\gamma^*d} = 2057, 2137, 2217, \text{ and } 2297 \text{ MeV}$, i.e., to the same pion momentum. The structure functions are shown in Figs. 4 and 5, respectively. Comparing the corresponding structure functions in both figures, one notices a qualitative similarity in the shape although they differ substantially in absolute size due to the considerably different momentum transfer. Thus we can limit the discussion to set B in Fig. 4. As above, f_L is dominated by the Born terms showing a sizable destructive interference between direct and crossed contributions. With increasing ω the absolute size increases and the forward peaking becomes more and more pronounced.

In f_T one clearly notices the increasing importance of the Δ contribution as is expected when crossing the Δ region. The panels at the two lowest energy transfers at $\omega = 130$ and 210 MeV show qualitatively the same behaviour as the panels for f_T at $\omega = 160$ and 200 MeV of set A in Fig. 3. Right on the Δ at $\omega = 290 \text{ MeV}$, they have almost no influence. Only above this region the Born terms become significant again and interfere destructively in the forward direction so that the forward peak moves to about 30 degree.

With respect to the interference structure functions, f_{LT} shows the same qualitative angular behaviour as for the set A for energy transfers below the Δ resonance region. However, on and above this region this is not true any more. There the Δ dominates and the Born terms contribute very little. The transverse interference structure function f_{TT} exhibits a different behaviour compared to set A at all energies. At the lowest energy of 130 MeV , one notices an almost complete cancellation between resonance and Born contributions. But already at 210 MeV the Born terms become relatively small, and at $\omega = 290 \text{ MeV}$ they are completely negligible while at higher energy transfers they start to show again some influence, although direct and crossed Born terms interfere destructively, but lead to a slight enhancement of the resonance contribution.

Altogether, all structure functions of sets B and C except f_L are dominated by the Δ over a large region of energy transfers crossing the resonance position. This was to be expected because of the dominance of the transverse Δ excitation current. Only f_L is governed by the Born terms, a fact which might be changed somewhat if the neglected small $C2$ contribution is included. But we do not expect drastic changes due to the smallness of such contributions. As to the absolute size, f_T is by far the largest below and on the resonance, followed by f_{TT} which becomes of the same size above the resonance. Sizeably smaller are f_L and f_{LT} .

We also have calculated the form factors F_L and F_T of the inclusive cross section for the sets B and C, because they allow a better comparison of the absolute values. They are shown in Figs. 6 and 7. For both sets the longitudinal form factor F_L shows a steady increase over the whole range of energy transfers considered which arises essentially from the e.m. form factor because one approaches the photon point with increasing ω . By destructive interference the direct Born contribution is reduced to about 30 percent via the crossed one. As noted before, the Δ is negligible here in contrast to the transverse form factor F_T . Here the direct and crossed Born contribution show a distinctly different behaviour. While the direct one leads only to a slight general increase of the Δ contribution, the crossed Born contribution results in a downshift of the maximum by about 20 MeV and a significant reduction above the maximum. In absolute size, F_T is about one to two orders of magnitude bigger than F_L . Comparing sets B and C one notices a decrease of the form factors by a factor of about 5 due to the higher four momentum transfers involved in set C.

Finally, we will consider in Fig. 8 the structure functions of set D at a constant energy transfer $\omega = 300 \text{ MeV}$ with varying three momentum transfers, which means close and slightly above the resonance region. Accordingly, one readily notices the angular behaviour which we had found before at corresponding kinematics. In f_L the destructive interference of direct and crossed Born terms becomes again apparent. For f_T one readily sees the increasing reduction of the forward Δ peak by the background contributions with increasing momentum transfer resulting in a small shift away from the forward direction. On the contrary, the interference structure functions show qualitatively very little variation with the momentum transfer. Only the absolute size decreases rapidly which is also the case for the diagonal structure functions f_L and f_T and for the corresponding inclusive form factors shown in Fig. 9. This is a consequence of the increasing four momentum transfer which governs the e.m. form factors of the elementary vertices.

V. SUMMARY AND CONCLUSIONS

Coherent π^0 electroproduction on the deuteron has been studied in the impulse approximation neglecting rescattering and two-body effects. For the elementary reaction on the nucleon, we have considered besides the dominant excitation of the $\Delta(1232)$ resonance the usual Born terms, essentially in the same frame work as in the analogous photo process. The four structure functions which govern the differential cross section have been evaluated along various cuts in the plane of energy-momentum transfer. In particular, the relative importance of the resonance and background contributions have been studied in detail. They show quite different influences in the different structure

functions, due to the fact, that the excitation of the Δ resonance proceeds dominantly via M1 excitations, which are purely transverse. It now remains as a task for the future to study the influence of rescattering and, furthermore, to use a more refined elementary production operator, in particular for the threshold region.

APPENDIX A: COMPLETENESS PROOF FOR THE BASIC OPERATOR SET

In this appendix we will present an independent proof that the operators listed in Table I form a complete and independent basis for the representation of the T -matrix of coherent e.m. pseudoscalar production on a spin-one target. Independence means that a relation

$$\sum_{\alpha} f_{\alpha}(k, q, \cos \theta) \mathcal{O}_{\alpha} \equiv 0 \quad (\text{A.1})$$

with $k = |\vec{k}|$, $q = |\vec{q}|$ and $\cos \theta = \hat{k} \cdot \hat{q}$, is fulfilled only if $f_{\alpha} \equiv 0$ for all α .

To this end we consider first an alternative set whose elements also have to be built out of the only available unit vectors \hat{k} and \hat{q} and the spin-one operators $S^{[\Sigma]}$ ($\Sigma = 0, 1, 2$). Explicitly these new operators have the form $\vec{O}_{(KQ)L}^{\Sigma} \cdot \vec{\epsilon}_{\mu}$ with

$$\vec{O}_{(KQ)L}^{\Sigma} := [A_{KQ}^{[L]} \times S^{[\Sigma]}]^{[1]}, \quad (\text{A.2})$$

where we have introduced

$$A_{KQ}^{[L]} := [k^{[K]} \times q^{[Q]}]^{[L]} \quad (\text{A.3})$$

with the following recursive definitions of the spherical tensors $a^{[n]}$

$$\begin{aligned} a^{[0]} &:= 1, \\ a^{[1]} &:= \hat{a}, \\ a^{[n+1]} &:= [a^{[1]} \times a^{[n]}]^{[n+1]}, \quad \forall n \in \mathbf{N}. \end{aligned}$$

They are related to the spherical harmonics by

$$a^{[n]} = \alpha_n Y^{[n]} \quad \text{with} \quad \alpha_n = \sqrt{\frac{4\pi n!}{(2n+1)!}}. \quad (\text{A.4})$$

Angular momentum coupling rules restrict the L -values in (A.2) to $|\Sigma - 1| \leq L \leq \Sigma + 1$. The possible combinations are listed in Table II. Furthermore, in order to insure that $\vec{O}_{(KQ)L}^{\Sigma}$ be a pseudo-vector, the condition $K + Q = \text{even}$ has to be fulfilled. Taking into account this condition and the coupling rules, one finds for the values of the indices K, Q, L the combinations listed in Table III.

As next we will derive a recursion relation for the $A_{KQ}^{[L]}$ based on the recoupling of the following expression

$$\begin{aligned} A_{NN}^{[0]} A_{KQ}^{[L]} &= [A_{NN}^{[0]} \times A_{KQ}^{[L]}]^{[L]} \\ &= \sum_{K_1=|K-N|}^{K+N} \sum_{Q_1=|Q-N|}^{Q+N} C_{NKQ}^{(K_1 Q_1) L} A_{K_1 Q_1}^{[L]}, \end{aligned} \quad (\text{A.5})$$

where

$$\begin{aligned} C_{NKQ}^{(K_1 Q_1) L} &= (-)^{N+L+K_1+Q} \frac{\hat{K}_1 \hat{Q}_1}{\hat{N}} \beta_{NK}^{K_1} \beta_{NQ}^{Q_1} \left\{ \begin{matrix} K & Q & L \\ Q_1 & K_1 & N \end{matrix} \right\}, \\ \beta_{AB}^C &= (-)^C \sqrt{\frac{A! B! (2C+1)!!}{(2A+1)!! (2B+1)!! C!}} \begin{pmatrix} A & B & C \\ 0 & 0 & 0 \end{pmatrix}. \end{aligned} \quad (\text{A.6})$$

One should note that $A_{NN}^{[0]}$ is basically the Legendre polynomial $P_N(\cos \theta)$, namely

$$A_{NN}^{[0]} = \alpha_N^2 \frac{(-)^N \hat{N}}{4\pi} P_N(\cos \theta). \quad (\text{A.7})$$

Separating in (A.5) on the rhs the term with the highest indices $K_1 = K + N$ and $Q_1 = Q + N$, one finds

$$\begin{aligned} A_{NN}^{[0]} A_{KQ}^{[L]} &= \sum_{K_1=|K-N|}^{K+N-1} \sum_{Q_1=|Q-N|}^{Q+N} C_{NKQ}^{(K_1 Q_1)L} A_{K_1 Q_1}^{[L]} \\ &+ \sum_{Q_1=|Q-N|}^{Q+N-1} C_{NKQ}^{((K+N) Q_1)L} A_{(K+N) Q_1}^{[L]} \\ &+ C_{NKQ}^{((K+N)(Q+N)L} A_{(K+N)(Q+N)}^{[L]}. \end{aligned} \quad (\text{A.8})$$

With the replacements $K + N \rightarrow K$ and $Q + N \rightarrow Q$ the above equation finally leads to the recursion relation

$$\begin{aligned} C_{N(K-N)(Q-N)}^{(KQ)L} A_{KQ}^{[L]} &= A_{NN}^{[0]} A_{(K-N)(Q-N)}^{[L]} \\ &- \sum_{K_1=|K-2N|}^{K-1} \sum_{Q_1=|Q-2N|}^Q C_{N(K-N)(Q-N)}^{(K_1 Q_1)L} A_{K_1 Q_1}^{[L]} \\ &- \sum_{Q_1=|Q-2N|}^{Q-1} C_{N(K-N)(Q-N)}^{(K Q_1)L} A_{K Q_1}^{[L]}. \end{aligned} \quad (\text{A.9})$$

Since K, Q and L have to fulfil the usual triangular relation N is limited by $N \leq \frac{1}{2}(K + Q - L)$. By this relation, $A_{KQ}^{[L]}$ is expressed as a linear superposition of $A_{K_1 Q_1}^{[L]}$ where $K_1 \leq K$, $Q_1 \leq Q$, and $K_1 + Q_1 < K + Q$.

According to Table III one has for $L \in \{0, 1\}$ only the combination $K = Q$. While for $L = 0$ the recursion formula becomes trivial

$$A_{NN}^{[0]} = A_{NN}^{[0]} A_{00}^{[0]}, \quad (\text{A.10})$$

one finds for $L = 1$

$$\begin{aligned} C_{N(K-N)(K-N)}^{(KK)1} A_{KK}^{[1]} &= A_{NN}^{[0]} A_{(K-N)(K-N)}^{[1]} \\ &- \sum_{K_1=|K-2N|}^{K-1} \sum_{Q_1=|K-2N|}^K C_{N(K-N)(K-N)}^{(K_1 Q_1)1} A_{K_1 Q_1}^{[1]} \\ &- \sum_{Q_1=|K-2N|}^{K-1} C_{N(K-N)(K-N)}^{(K Q_1)1} A_{K Q_1}^{[1]}. \end{aligned} \quad (\text{A.11})$$

Exploiting the properties of the coefficients $C_{NKQ}^{(K_1 Q_1)L}$ ($N + K + K_1$ and $N + Q + Q_1$ must both be even numbers while K_1, Q_1 and 1 must obey the triangular relation) (A.11) simplifies to

$$C_{N(K-N)(K-N)}^{(KK)1} A_{KK}^{[1]} = A_{NN}^{[0]} A_{(K-N)(K-N)}^{[1]} - \sum_{K_1=|K-2N|}^{K-2} C_{N(K-N)(K-N)}^{(K_1 K_1)1} A_{K_1 K_1}^{[1]}. \quad (\text{A.12})$$

Setting $N = 1$, one finds

$$C_{1(K-1)(K-1)}^{(KK)1} A_{KK}^{[1]} = A_{11}^{[0]} A_{(K-1)(K-1)}^{[1]} - C_{1(K-1)(K-1)}^{((K-2)(K-2)1} A_{(K-2)(K-2)}^{[1]}, \quad (\text{A.13})$$

from which readily follows that $A_{11}^{[1]}$ is the only initial element of the recursion for $L = 1$ as was $A_{00}^{[0]}$ for $L = 0$. Thus every $A_{KK}^{[1]}$ is related to $A_{11}^{[1]}$ times a function in $\cos \theta$.

Proceeding in complete analogy, we obtain for $L = 2$ and $N = 1$

$$\begin{aligned}
C_{1(K-1)(Q-1)}^{(KQ)2} A_{KQ}^{[2]} &= A_{11}^{[0]} A_{(K-1)(Q-1)}^{[2]} - \sum_{K_1=|K-2|}^{K-1} \sum_{Q_1=|Q-2|}^{Q-1} C_{1(K-1)(Q-1)}^{(K_1 Q_1)2} A_{K_1 Q_1}^{[2]} \\
&\quad - \sum_{K_1=|K-2|}^{K-1} C_{1(K-1)(Q-1)}^{(K_1 Q)2} A_{K_1 Q}^{[2]} - \sum_{Q_1=|Q-2|}^{Q-1} C_{1(K-1)(Q-1)}^{(K Q_1)2} A_{K Q_1}^{[2]}, \tag{A.14}
\end{aligned}$$

respectively,

$$\begin{aligned}
C_{1(K-1)(Q-1)}^{(KQ)2} A_{KQ}^{[2]} &= A_{11}^{[0]} A_{(K-1)(Q-1)}^{[2]} - C_{1(K-1)(Q-1)}^{((K-2)(Q-2))2} A_{(K-2)(Q-2)}^{[2]} \\
&\quad - C_{1(K-1)(Q-1)}^{((K-2)Q)2} A_{(K-2)Q}^{[2]} - C_{1(K-1)(Q-1)}^{(K(Q-2))2} A_{K(Q-2)}^{[2]}. \tag{A.15}
\end{aligned}$$

As independent elements one finds here $A_{11}^{[2]}$, $A_{20}^{[2]}$, $A_{02}^{[2]}$ which cannot be further reduced. In other words, every $A_{KQ}^{[2]}$ can be expressed as a linear combination of these independent elements with appropriate functions in $\cos\theta$ as coefficients. An analogous relation holds for $L = 3$

$$\begin{aligned}
C_{1(K-1)(Q-1)}^{(KQ)3} A_{KQ}^{[3]} &= A_{11}^{[0]} A_{(K-1)(Q-1)}^{[3]} - C_{1(K-1)(Q-1)}^{((K-2)(Q-2))3} A_{(K-2)(Q-2)}^{[3]} \\
&\quad - C_{1(K-1)(Q-1)}^{((K-2)Q)3} A_{(K-2)Q}^{[3]} - C_{1(K-1)(Q-1)}^{(K(Q-2))3} A_{K(Q-2)}^{[3]}. \tag{A.16}
\end{aligned}$$

Here the remaining independent elements are $A_{22}^{[3]}$, $A_{31}^{[3]}$, $A_{13}^{[3]}$. With this we finally have proven that the set of operators listed in Table IV is independent and complete.

Although these basic elements do not separate in general into transverse and longitudinal operators this set provides a better starting point for a systematic (computer aided) decomposition of the amplitude. The transition to the transverse and longitudinal operators of Table I can then be obtained by the following transformation

$$\begin{aligned}
\mathcal{O}_{T,1} &= -i\sqrt{2} \mathcal{O}_1, \\
(\mathcal{O}_{T,2}, \mathcal{O}_{T,3}, \mathcal{O}_{T,4}, \mathcal{O}_{L,1}, \mathcal{O}_{L,2})^T &= \mathcal{A} \cdot (\mathcal{O}_2, \mathcal{O}_3, \mathcal{O}_4, \mathcal{O}_5, \mathcal{O}_6)^T, \\
(\mathcal{O}_{T,5}, \mathcal{O}_{T,6}, \mathcal{O}_{T,7}, \mathcal{O}_{T,8}, \mathcal{O}_{T,9}, \mathcal{O}_{L,3}, \mathcal{O}_{L,4})^T &= \mathcal{B} \cdot (\mathcal{O}_7, \mathcal{O}_8, \mathcal{O}_9, \mathcal{O}_{10}, \mathcal{O}_{11}, \mathcal{O}_{12}, \mathcal{O}_{13})^T. \tag{A.17}
\end{aligned}$$

with the transformation matrices

$$\begin{aligned}
\mathcal{A} &= \begin{pmatrix} \frac{2(1-P_2(\cos\theta))}{9} & 0 & -\frac{2\sqrt{5}}{\sqrt{3}} \cos\theta & \sqrt{\frac{5}{3}} & \sqrt{\frac{5}{3}} \\ -\frac{2}{3} & 0 & 0 & 0 & -\sqrt{\frac{5}{3}} \\ -\frac{2}{3} \cos\theta & -1 & -\sqrt{\frac{5}{3}} & 0 & 0 \\ \frac{1}{3} & 0 & 0 & 0 & -\sqrt{\frac{5}{3}} \\ \frac{1}{3} \cos\theta & 1 & -\sqrt{\frac{5}{3}} & 0 & 0 \end{pmatrix}, \tag{A.18} \\
\mathcal{B} &= \begin{pmatrix} -\frac{i\sqrt{2}}{\sqrt{15}} & -\frac{i\sqrt{10}}{3} & 0 & \frac{i\sqrt{10}}{3} \cos\theta & 0 & 0 & -\frac{i\sqrt{28}}{3} \\ -\frac{i\sqrt{2}}{\sqrt{15}} \cos\theta & 0 & -\frac{i\sqrt{5}}{3\sqrt{2}} & \frac{i\sqrt{5}}{3\sqrt{2}} & -\frac{i\sqrt{7}}{\sqrt{3}} & 0 & 0 \\ -\frac{i\sqrt{2}}{\sqrt{15}} & \frac{i\sqrt{10}}{3} & \frac{i\sqrt{10}}{3} \cos\theta & 0 & 0 & -\frac{i\sqrt{28}}{3} & 0 \\ 0 & 0 & 0 & -\frac{i\sqrt{3}}{\sqrt{2}} & 0 & 0 & 0 \\ \frac{i}{\sqrt{2}} & -\frac{i3\sqrt{5}}{\sqrt{2}} & 0 & 0 & 0 & 0 & 0 \\ -\frac{i3}{2\sqrt{2}} & -\frac{i(3\sqrt{15}-4)}{\sqrt{360}} & 0 & -\frac{i\sqrt{5}}{3\sqrt{2}} \cos\theta & 0 & 0 & -\frac{i\sqrt{28}}{3} \\ \frac{i\sqrt{3}}{\sqrt{10}} \cos\theta & -\frac{i\sqrt{5}}{\sqrt{2}} \cos\theta & -\frac{i\sqrt{5}(\sqrt{3}-1)}{3\sqrt{2}} & \frac{i\sqrt{5}}{3\sqrt{2}} & -\frac{i\sqrt{7}}{\sqrt{3}} & 0 & 0 \end{pmatrix}. \tag{A.19}
\end{aligned}$$

[1] F.X. Lee, L.E. Wright, and C. Bennhold, Phys. Rev. C **55**, 318 (1997).

- [2] M. Effenberger, A. Hombach, S. Teis, and U. Mosel, Nucl. Phys. A **614**, 501 (1997).
[3] K.I. Blomqvist et al., Nucl. Phys. A **626**, 871 (1997).
[4] P. Hoffmann-Rothe et al., Phys. Rev. Lett. **78**, 4697 (1997).
[5] M. Liang et al., Phys. Lett. B **411**, 244 (1997).
[6] H. Merkel, Lecture Notes in Physics, Vol. **513**, 114 (1998).
[7] M.P. Rekalo and I.V. Stoletnii, J. Phys. G **17**, 1643 (1991).
[8] F. Blaazer, B.L.G. Bakker, and H.J. Boersma, Nucl. Phys. A **568**, 681 (1994).
[9] H. Garcilazo and E. Moya de Guerra, Phys. Rev. C **49**, R601 (1994).
[10] P. Wilhelm, H. Arenhövel, Nucl. Phys. A **593**, 435 (1995).
[11] P. Wilhelm, H. Arenhövel, Nucl. Phys. A **609**, 469 (1996).
[12] S.S. Kamalov, L. Tiator, and C. Bennhold, Phys. Rev. C **55**, 98 (1997).
[13] B.K. Jeon, T. Sato, and H. Ohtsubo, Phys. Lett. B **228**, 304 (1989).
[14] H. Arenhövel, Few-Body Syst. **25**, 157 (1998).
[15] U. Fano and G. Racah, *Irreducible Tensorial Sets* (Academic Press, New York 1959)
[16] E. Breitmoser and H. Arenhövel, Nucl. Phys. A **612**, 321 (1997).
[17] R. Machleidt, K. Holinde, and C. Elster, Phys. Rep. **149**, 1 (1987).

TABLE I. Basic set of independent, nonrelativistic transverse and longitudinal operators, where $\hat{k} = \vec{k}/|\vec{k}|$ and $\hat{q} = \vec{q}/|\vec{q}|$.

β	$\mathcal{O}_{T,\beta}$	$\mathcal{O}_{L,\beta}$
1	$\vec{\epsilon} \cdot (\hat{k} \times \hat{q})$	$\hat{k} \cdot \vec{S}$
2	$\vec{\epsilon} \cdot (\hat{k} \times \hat{q}) (\hat{k} \times \hat{q}) \cdot \vec{S}$	$\hat{q} \cdot \vec{S}$
3	$\vec{\epsilon} \cdot (\hat{k} \times (\hat{k} \times \vec{S}))$	$[(\hat{k} \times \hat{q}) \times \hat{k}]^{[2]} \cdot S^{[2]}$
4	$\vec{\epsilon} \cdot (\hat{k} \times (\hat{q} \times \vec{S}))$	$[(\hat{k} \times \hat{q}) \times \hat{q}]^{[2]} \cdot S^{[2]}$
5	$\vec{\epsilon} \cdot (\hat{k} \times \hat{q}) \hat{k}^{[2]} \cdot S^{[2]}$	
6	$\vec{\epsilon} \cdot (\hat{k} \times \hat{q}) [\hat{k} \times \hat{q}]^{[2]} \cdot S^{[2]}$	
7	$\vec{\epsilon} \cdot (\hat{k} \times \hat{q}) \hat{q}^{[2]} \cdot S^{[2]}$	
8	$\vec{\epsilon} \cdot (\hat{k} \times [\hat{k} \times S^{[2]}]^{[1]})$	
9	$\vec{\epsilon} \cdot (\hat{k} \times [\hat{q} \times S^{[2]}]^{[1]})$	

TABLE II. Possible values of L and Σ of the operators in (A.3).

Σ	0	1	2
L	1	0 1	1 2 3

TABLE III. Listing of possible (KQL) combinations.

L	K	Q
0,1	$K \geq 0$	K
2	0	2
	1	1,3
	$K \geq 2$	$K - 2, K, K + 2$
3	$K < 3$	$K + 2$
	$K \geq 3$	$K - 2, K, K + 2$

TABLE IV. Listing of the 13 basic operators $\mathcal{O}_\alpha = \vec{O}_{(KQ)L}^\Sigma \cdot \vec{\epsilon}_\mu$.

α	1	2	3	4	5	6	7	8	9	10	11	12	13
Σ	0	1	1	1	1	1	2	2	2	2	2	2	2
L	1	0	1	2	2	2	1	2	2	2	3	3	3
K	1	0	1	1	0	2	1	1	0	2	2	1	3
Q	1	0	1	1	2	0	1	1	2	0	2	3	1

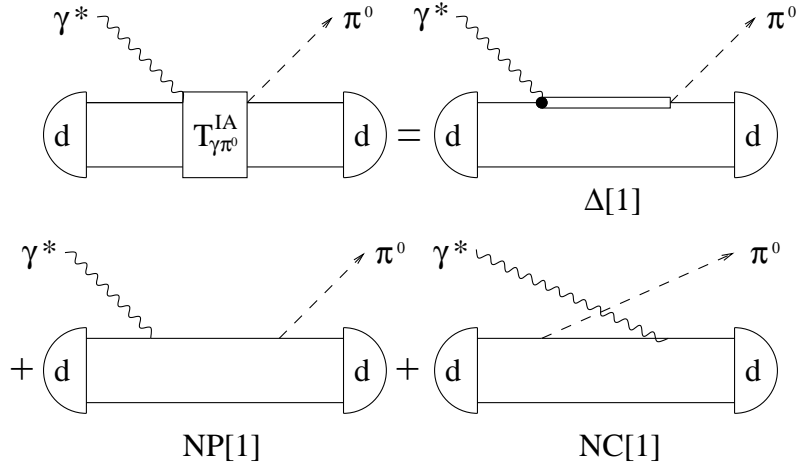


FIG. 1. Impulse approximation diagrams for $\gamma^* + d \rightarrow \pi^0 + d$ with resonance contribution $\Delta[1]$, direct NP[1] and crossed NC[1] nucleon pole contribution.

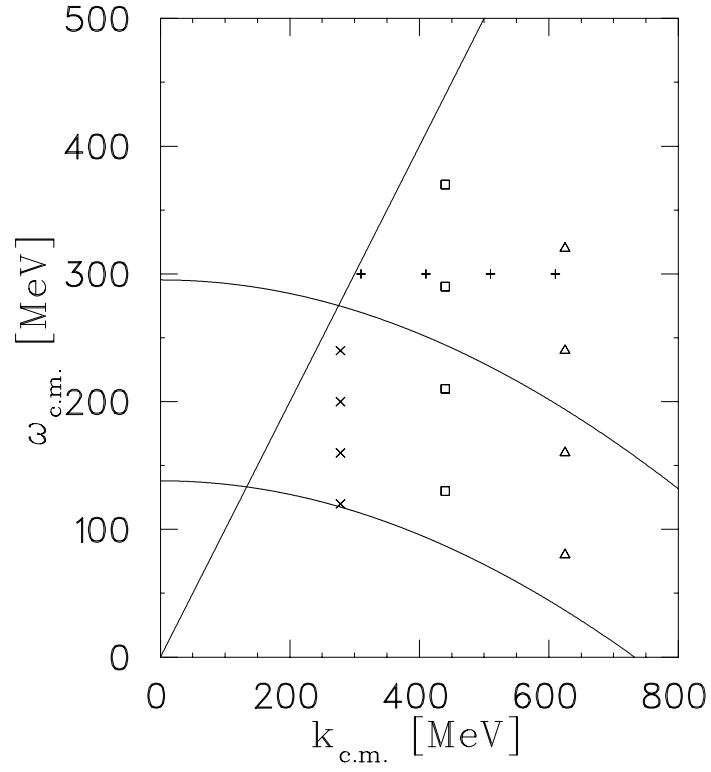


FIG. 2. Various sets of kinematics in the k - ω -plane chosen for the numerical evaluation, labeled A (\times), B (\square), C (\triangle) and D ($+$). The straight line represents the photon line. The lower curve marks the π^0 production threshold while the upper curve represents the location of the Δ -resonance.

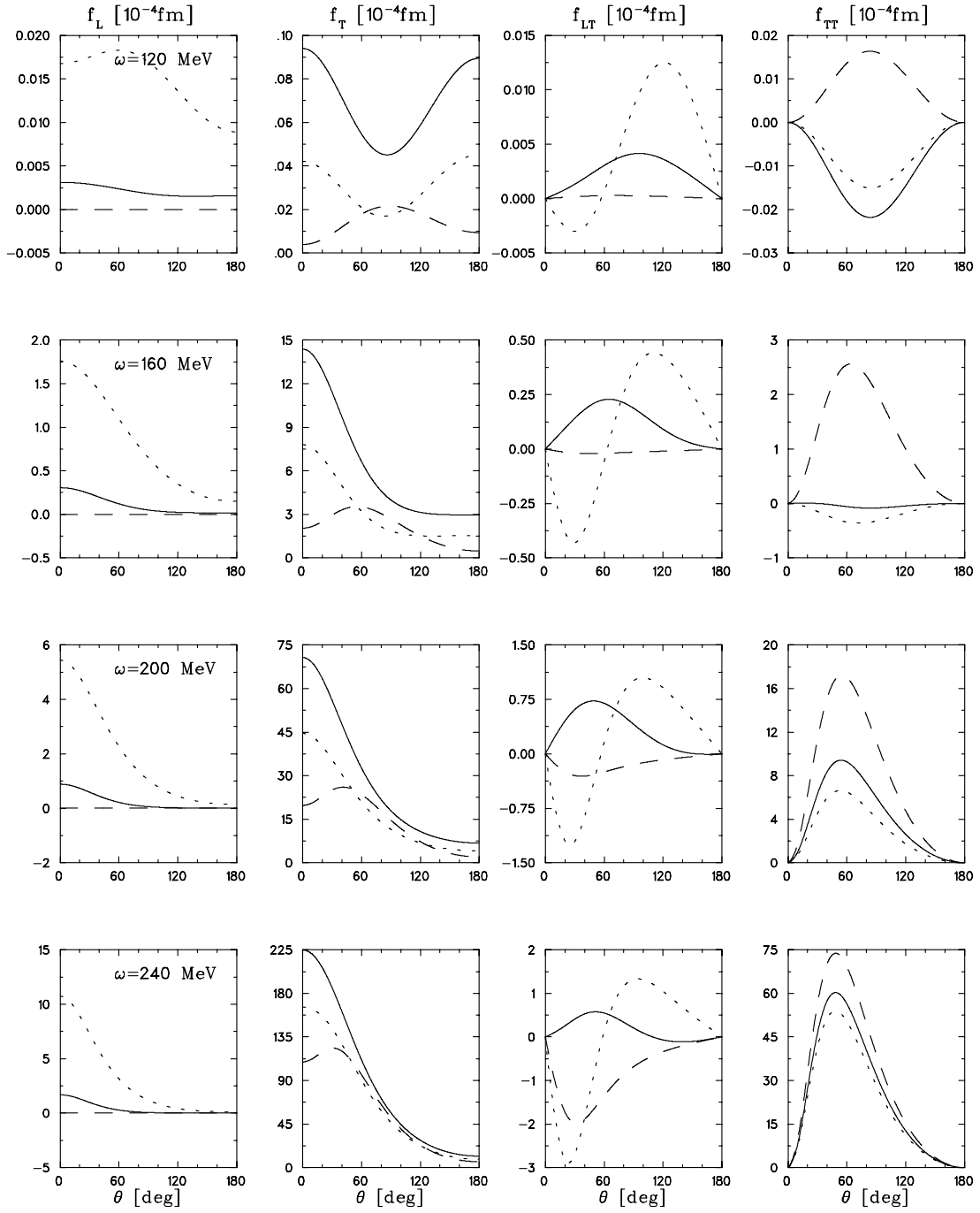


FIG. 3. Structure functions for the set A at constant momentum transfer $k^2 = 2 \text{ fm}^{-2}$ for various energy transfers. Dashed curves: pure Δ contribution; dotted curves: direkt Born term added; full curves: complete IA.

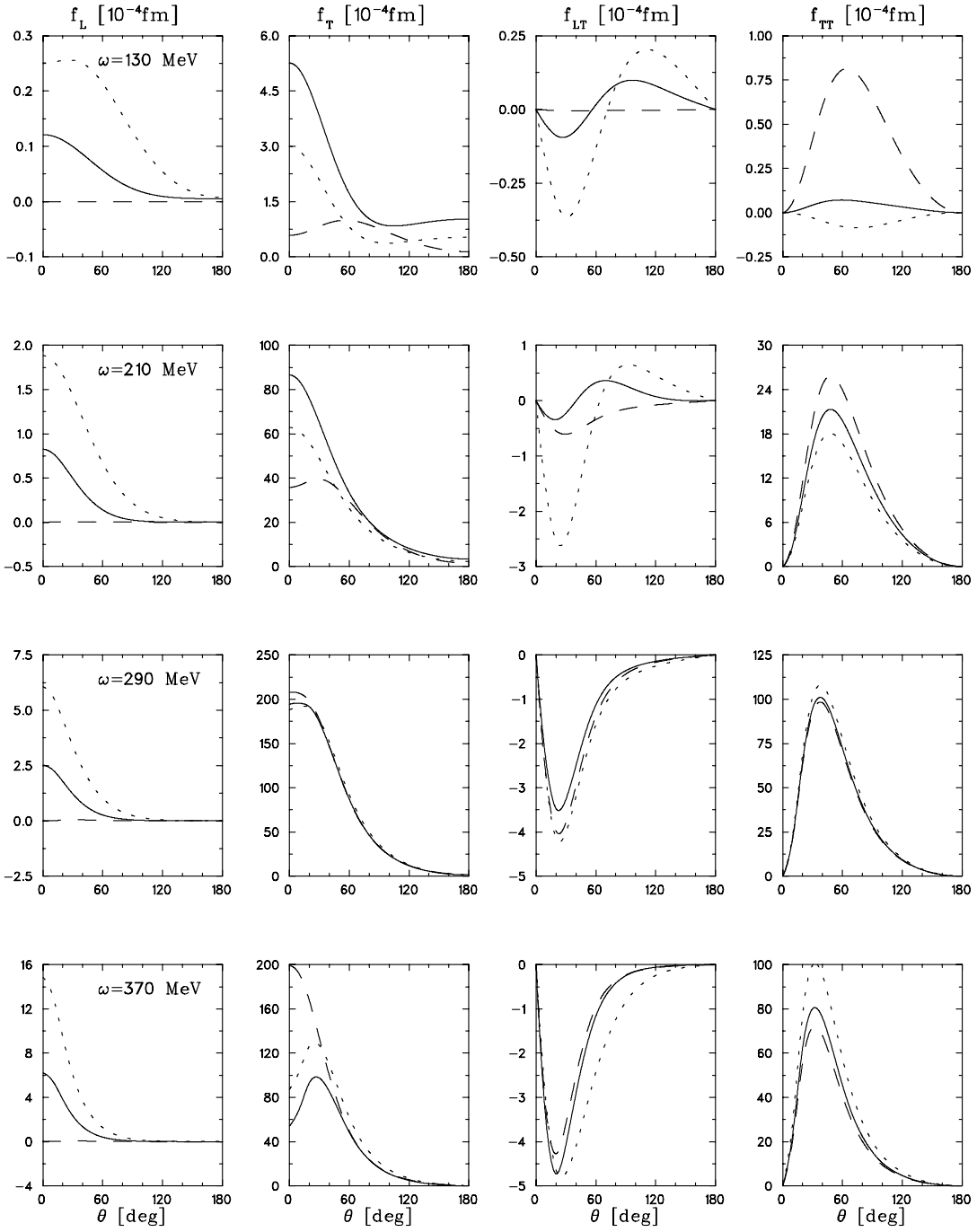


FIG. 4. Structure functions for the set B at constant momentum transfer $k^2 = 5 \text{ fm}^{-2}$ for various energy transfers. Notation as in Fig. 3.

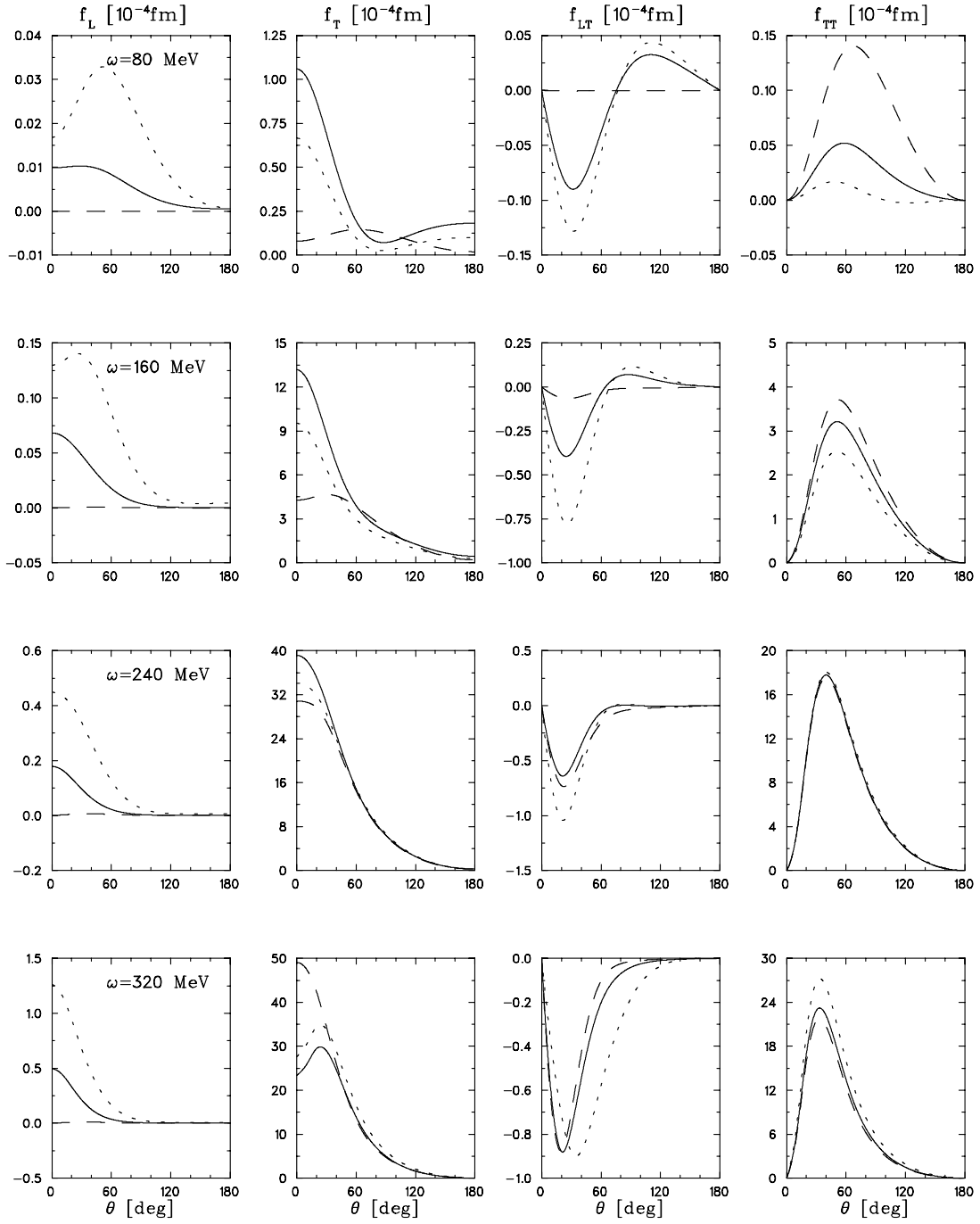


FIG. 5. Structure functions for the set C at constant momentum transfer $k^2 = 10 \text{ fm}^{-2}$ for various energy transfers. Notation as in Fig. 3.

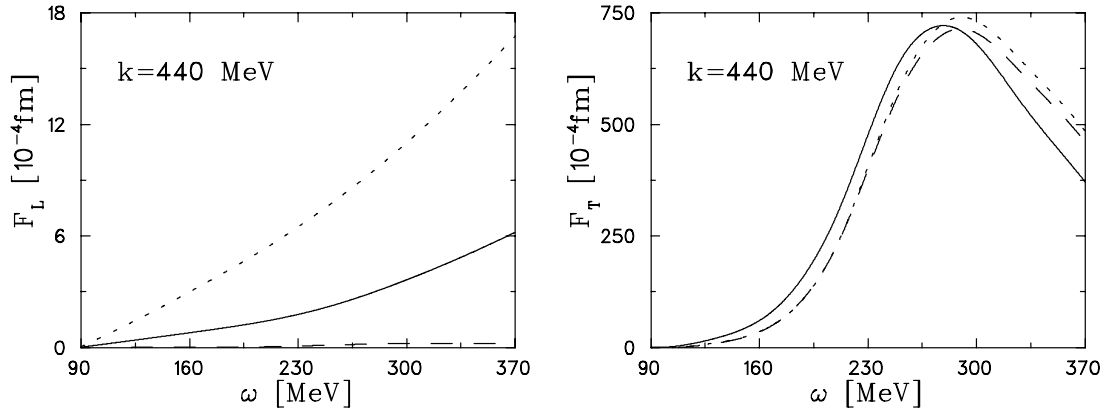


FIG. 6. Longitudinal and transverse form factors for set B. Notation as in Fig. 3.

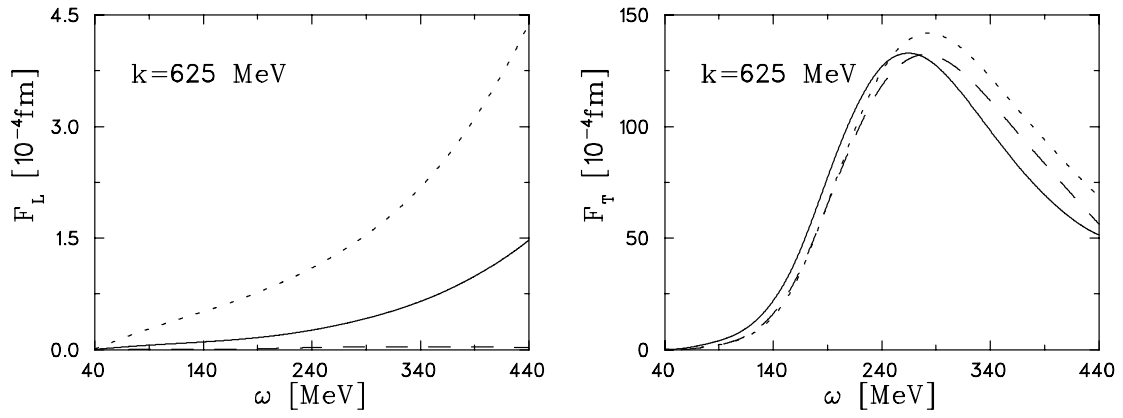


FIG. 7. Longitudinal and transverse form factors for set C. Notation as in Fig. 3.

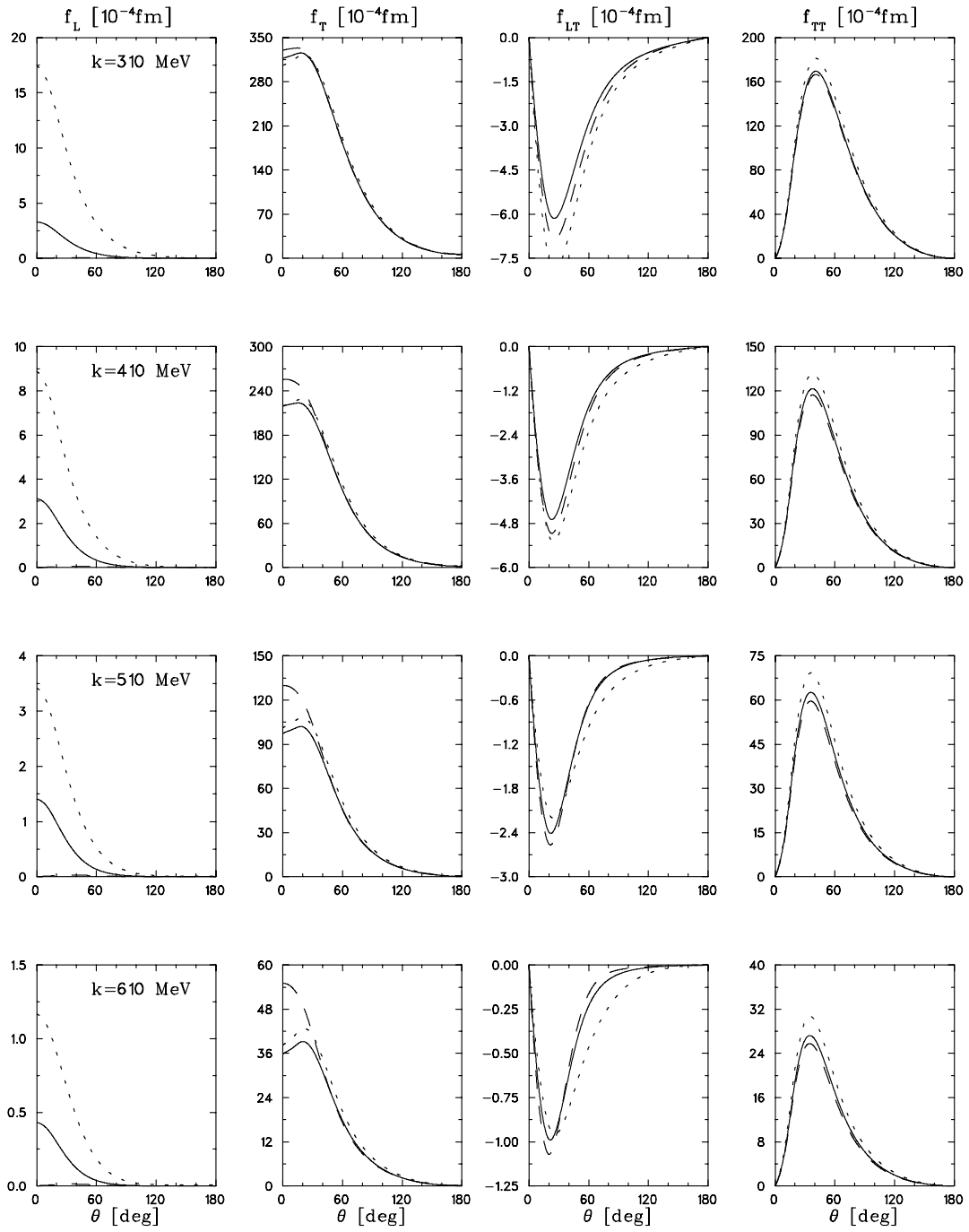


FIG. 8. Structure functions for the set D at constant energy transfer $\omega = 300$ MeV for various momentum transfers. Notation as in Fig. 3.

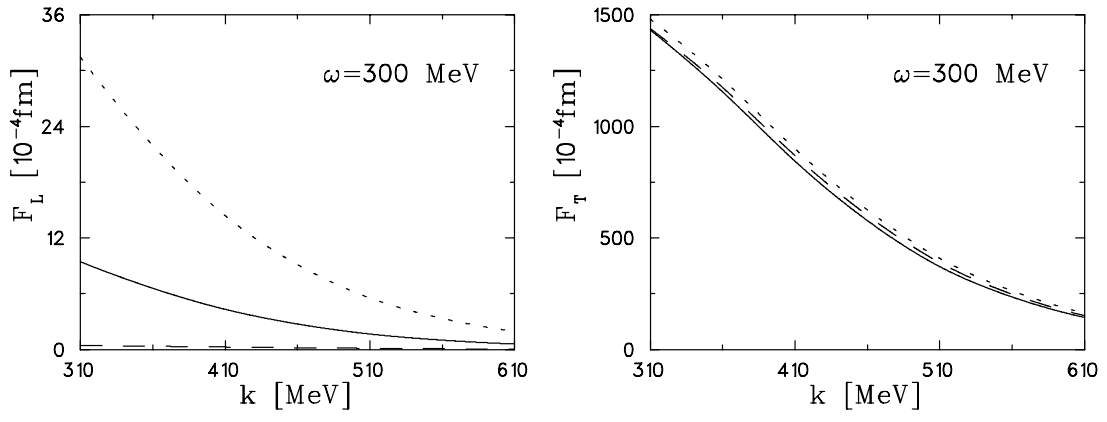


FIG. 9. Longitudinal and transverse form factors for set D. Notation as in Fig. 3.